Feasibility study of low-carbon ammonia and steel production in Europe

J-L. HOXHA[1,*], M. CASPAR[1,*], A. DONCEEL[1,*], J. FRASELLE[1,*], M. PHILIPPART de FOY[1,*] and R. PONCELET[1,*]

[1] *Authors have equally contributed to this work.*
[*] *Master students, Department of Chemical Engineering, ULiège, Belgium*

Abstract— In Europe, industrial processes currently account for a significant share of the energy demand (25%) and associated emissions of carbon dioxide (17%). In the coming years, the concentration of CO_2 in the atmosphere will continue to increase critically. As stipulated in the Paris Agreement, greenhouse gas emissions have to be reduced in order to maintain the global warming well below 2°C. This will require shifting industrial production currently based on fossil energies towards the use of renewable energies. Regarding these new energetic opportunities, the present article considers two conceptual chemical processes that may operate in Europe with really low carbon emissions through the use of green hydrogen. The studied processes are projections of the production of ammonia and steel in the 2030s. With hydrogen as raw material, their CO_2 emissions could be drastically decreased. This hydrogen is produced by water electrolysis with Proton Exchange Membrane electrolysers (PEMEC). It is assumed that the electricity required by the processes is entirely supplied from renewable energies. This allows to obtain the desired products in a decarbonised way. The objective of the present study is to show that it will be possible to design low-carbon emission processes in a close future. Based on current industrial sectors of both ammonia and steel productions, detailed modellings of the two decarbonised processes in `Aspen Plus` software are proposed. In order to prove the feasibility of these processes, an economic analysis is also presented.

Keywords—Ammonia, Steel, Electrolysis, Green, Hydrogen, Renewable.

INTRODUCTION

The environmental changes encountered nowadays are more and more worrying. Urgent measures need to be adopted and fundamental modifications are required, including in the chemical sector. In Europe, industrial processes currently account for a significant share of the energy demand (25%) [1] and associated emissions of carbon dioxide (17%) [2]. As stipulated in the Paris Agreement, greenhouse gas emissions have to be reduced in order to maintain the global warming well below 2°C. Moreover, the European Union committed to become carbon neutral by 2050 [3]. This will require shifting the industrial production currently based on fossil energies towards the use of renewable energies. A thorough study of these processes should be carried out with the aim of reducing emissions. Green hydrogen could help to reach that goal.

This article details two hydrogen consuming processes that are adapted to use a feed of pure H_2 produced by electrolysis with renewable energy. Those processes should be examples of what the chemical plants will become in the next decades if environmental policies are followed. The two cases that are studied in this article are the production of ammonia and the steelmaking process. Currently, those processes exist but emit important amounts of greenhouse gases due to their consumption of fossil fuels. The goal of this work is to study the feasibility of a transition to very low-CO_2 emission processes and to see what assumptions have to be made to reach that objective.

The present work includes a literature review of the current processes and available technologies, details the modellings of the two processes using pure hydrogen and ends with the cost analysis of the two systems. All the developments are coupled with discussions on the viability of the processes.

This work was written in the scope of the "Student contest problem 2019" organised by Eurecha [4, 5] and so considers production sites situated in Europe.

LITERATURE REVIEW

A literature review is conducted on the existing processes and the state of the art technologies. It focuses on ammonia plants, production of steel and electrolyser technologies. The current processes emit large amounts of CO_2. Indeed, the H_2 consumed by the ammonia synthesis is produced by natural gas reforming or coal gasification and the reducing mixture used to reduce the iron ore in steelmaking comes mainly from coal gasification or, for some technologies, from natural gas.

Ammonia production

Currently, ammonia is mainly produced with the Haber-Bosh process, using the exothermic main reaction:

$$N_2 + 3\ H_2 \rightarrow 2\ NH_3\ (\Delta H_{298K} = -45.7\ \text{kJ/mol}_{NH_3})\ [6] \quad (1)$$

Air is used as source of N_2 while H_2 is usually produced

by natural gas reforming in Europe. The reforming of natural gas also produces CO with the reaction (2), which is converted into H_2 in a water gas shift reactor following the reaction (3). A decarbonisation step is required to capture the CO_2 emitted during this reaction:

$$CH_4 + H_2O \rightarrow CO + 3\,H_2 \ (\Delta H_{298K} = 206.2\ \text{kJ/mol}_{CH_4}) \quad (2)$$

$$CO + H_2O \rightarrow CO_2 + H_2 \ (\Delta H_{298K} = -41.1\ \text{kJ/mol}_{CO}) \quad (3)$$

The two reactants are then mixed in a catalytic reactor to form ammonia that is further separated by successive liquid-vapour separators. Liquid ammonia is obtained and the vapour containing the H_2 and N_2 that have not reacted is recycled to the entrance of the reactor. The reaction is usually conducted at high temperature and pressure, in ranges of 350-600°C and 150-400 bar [7, 8, 9]. α-Fe catalysts are used for the principal reaction. They are made of magnetite (Fe_3O_4) promoted with irreducible oxides such as K_2O or Al_2O_3 [8].

The market of ammonia was estimated to more than 140 million tons in 2018 [10] and the average size of a production site is 540 000 tons per year [11]. One ton of NH_3 was sold at 350 € in 2019 [12], which gave a total market of 49 billion € in 2019. Ammonia is mainly produced in China as the country produces 31% of the world production, and in Russia and US, with respectively 10% and 9% [10]. Europe produces 10% of the ammonia market and Germany is the most important European producer as it represents 17% of the continent's production [13].

The investment needed for an ammonia plant using natural gas as raw material is divided into several parts. The primary and secondary reforming parts represent 25% of the CAPEX, heat recuperation and conversion from CO to CO_2 respectively 10 and 4% and the decarbonisation process counts for 8% of the investment cost. The synthesis step only represents 20% of the CAPEX [14]. Moreover, the most emitting part of the ammonia process is the natural gas reforming required to produce the H_2. Indeed, for 1 ton of ammonia produced, 1.8 tons of CO_2 are emitted by a standard plant [4]. It is thus clear that using pure hydrogen as raw material would be a very interesting alternative to the current gas reforming step of the process. It would allow to hugely decrease the CO_2 emissions, as H_2 is produced with renewable energies, and the investment for the important CAPEX of the reforming part could be avoided. The transition to the use of H_2 from electrolysis is thus a relevant possibility that needs to be considered in the scope of the decarbonisation of ammonia plants.

Steelmaking

The production of steel in the world increases every year. 1.7 Gt of steel were produced in 2017, which corresponds to an increase of 5.3% compared to 2016 [15].

The purpose of the steelmaking process is to reduce iron ore, which is mainly composed of hematite (Fe_2O_3). Two ways exist in industry: blast furnace (BF) followed by basic oxygen furnace (BOF) or production of direct reduced iron (DRI) followed by electric arc furnace (EAF). It is also possible to use only the EAF when recycling scrap. Nevertheless, the BF+BOF route is the main one. All the existing DRI processes have produced 87 Mt of steel in 2017, which corresponds to 5 % of the overall steel production [16, 17].

In the BF+BOF process, iron ore pellets enter at the top of a blast furnace. Hot coke, made from coal, enters at the bottom of the furnace and is converted into CO and energy. The iron ore is melted and reduced as it is combined with the carbon released by the coke gasification. Limestone is also added at the top of the column, melts in the furnace and carries the coke ashes and impurities away from the furnace. The obtained pig iron enters then a basic oxygen furnace where it can potentially be mixed with scrap steel. The amount of scrap in a BOF cannot exceed 30% of the total charge as the heat required to melt the scrap is provided by the hot pig iron. The desired composition of the final steel can be reached by adapting the temperature in the furnace and the amount of scrap steel. [18].

The principle of the DRI process is to directly reduce the iron ore with H_2 and CO while the ore is still solid. The reducing agent is a mixture of CO and H_2 in 80% of the DRI production processes [16]. This mixture is produced by natural gas reforming. Other technologies are based on coke and use only CO as reductant. The reaction of reduction produces water and CO_2 as by-products. Those components leave the reactor with the remaining hydrogen by the top of the shaft while the reduced iron exits at its bottom.

The reduced iron can be transformed into hot briquetted iron (HBI) in order to store it or sell it. HBI can also be fed quickly to an EAF. If the direct reduced iron leaves the process as pellet, it can either be fed directly into an EAF as hot direct reduced iron (HDRI) or be cooled to prevent its oxidation and be stored as cold direct reduced iron (CDRI). Nevertheless, CDRI oxidises faster than HBI as its specific area is greater.

Midrex and *Energiron* are common DRI technologies that use the mixture of H_2 and CO as reducing agent. In those processes, the top outlet stream of the shaft is recycled as it contains a lot of H_2 and CO. Nevertheless, there are also impurities in this flow. Water and CO_2 have to be removed to avoid their accumulation. Water can easily be removed with a flash tank after the cooling of the flow. CO_2 can be separated by different methods: catalyst adsorption, solvent absorption, membrane separation or cryogenic separation [19].

Pressure swing adsorption (PSA) is the most common method. The gas is compressed to a pressure where CO_2 and other impurities are adsorbed on zeolites while hydrogen passes through the catalyst bed and leaves the vessel. The pressure of the equipment is then reduced to desorbe the impurities. As the adsorption process is promoted at low temperature, the vessel cannot exceed 200°C. Nevertheless, it is not a problem as the flow has to be cooled first to remove the water. This method is very common because it does not require any solvent and it consumes less energy than the cryogenic separation. However, the PSA method is quite expensive.

An alternative to PSA is the membrane separation. Different gases diffuse through a membrane, but their diffusion speeds are different. Therefore, the gases can be separated. This technique is cheaper than the PSA and could lead to very efficient separation. Unfortunately, the membrane separation technology is only studied at the laboratory scale currently

and will not be available for large scale plants in 2030 [20, 21, 22, 23].

The EAF allows the production of steel from HBI, HDRI or scrap. The reduced iron is melted with carbon, scrap and limestone. CaO is used as a slag former. The slag removes most of the impurities present in the melt. There are two other outlets of the EAF: fumes and steel. Fumes are mainly composed of CO and can be burnt in order to produce heat. The EAF is a batch process composed of three steps: charging and melting, refining and tapping. In order to be integrated into a continuous process, one EAF works with several buckets, each of them on a different stage of the process. It allows to have a period of time between two successive tappings of around 1 h [24, 25].

There is very limited literature on processes operating mainly with hydrogen. Indeed, CO is historically used as the main reductant in steel production. Nevertheless, the use of H_2 has advantages. First, the kinetic rate is faster with this component. This could lead to smaller reactors or higher production rates. However, the reaction is globally endothermic with hydrogen while it is exothermic with CO. Therefore, processes based on H_2 require more energy. The use of hydrogen can also lead to a sharp decrease of the CO_2 emission. Indeed, water is produced when this reductant is used while CO_2 is generated when CO is used. Conventional BF+BOF route processes emit around 2000 kg_{CO_2}/t_{steel} [26].

Electrolysis

In the present work, pure H_2 is substituted to conventional fossil fuels in both processes. This pure feed allows to avoid most of the CO_2 emissions as the natural gas reforming step or the coal gasification step is removed. Pure hydrogen and pure oxygen are produced from water electrolysis, as described by the reaction (4). The electricity required can be provided by renewable energies.

$$2\,H_2O \rightarrow 2\,H_2 + O_2 \;(\Delta H_{298K} = 286\ \text{kJ/mol}_{H_2O}) \quad (4)$$

Many electrolysers exist on the market, each having specific characteristics. Three types of electrolysis cells (EC) are investigated: Alkaline (AEC), Proton Exchange Membrane (PEMEC) and Solid Oxide Electrolysis (SOEC) [27].

The AEC is the most commonly used electrolyser in the industry. It consists in two electrodes that lay in a KOH solution separated by a membrane. Pure water is fed to the cell and the electrolyte OH^- crosses the membrane [28]. The yield of such a cell, *i.e.* the energy stored in the produced H_2 divided by the amount of electricity consumed, is close to 70%. Nevertheless, this yield could reach 85% by 2030 [29]. This type of electrolysis cell can work under conditions up to 30 bars and 70°C. The AEC is the most mature electrolyser available on the market today [27, 29, 30] and the least expensive technology, with a CAPEX of around 1000 €/kW [31], but its major drawback is its inflexibility to dynamic operations. Indeed, frequent start-ups or changes of the power input can negatively affect its efficiency [27].

A second type of electrolyser is the PEMEC. It operates in liquid phase, the electrolyte is H^+ and it is based on the concept of solid polymer electrolyte [28]. The operating conditions are around 70 to 90°C and it can work under a few hundred bar [29]. A high purity of water is required [27]. It is a less mature technology than the AEC and is still used mainly for small-scale applications, but its yield is supposed to reach 85% in 2030 for larger installations [27, 29, 30, 32]. It is a more expensive technology than the AEC as its capital cost is estimated at 2000 €/kW [31].

The last electrolyser considered is the SOEC. It operates in the gaseous phase with O^{2-} as electrolyte. The SOEC only operates at high temperature, around 800°C, and has a high efficiency of 85% due to the reaction in the gaseous phase. This type of cell is not developed at industrial scale and is still in the laboratory phase, but it has already shown conclusive results [27, 29, 30, 33]. Its CAPEX is similar to the CAPEX of the PEMEC, around 2000 €/kW [31].

The choice of electrolyser used to produce the required amount of H_2 is based on the characteristics of each technology, considering the fact that the electricity used for its functioning comes from renewable energies so there might be fluctuations of the supply. Given the specific application of the electrolysers in the studied processes, the choice of the technology is made regardless of their capital costs.

First, the AEC cannot be used for this application as it cannot cope with flexible electricity inputs without a huge decrease of its performances.

Then, even if the SOEC technology is promising, one major problem is encountered: the electrolyser needs to be continuously at 800°C. Contrary to the AEC, the SOEC does not need to operate continuously to keep a good yield, but the cell would be damaged if repeated heating and cooling occurred during the operating and stand-by alternations [34]. To avoid this problem, a heating device would be needed to keep a high temperature, even during periods where the SOEC is not operating.

To avoid the expenses due to this heater, the PEMEC is chosen. Even if this type of electrolyser is still in development, it can be assumed that in 2030, when the project starts, the technology will be available with an efficiency of 85% [29]. The PEMEC can operate above its nominal value but the efficiency decreases [34], and it appears to be the best-suited technology for fluctuating operations [31].

PROCESSES MODELLING

In this section, the models used for each process are detailed, including the design of the main equipment and the heat integration. The processes are modelled with `Aspen Plus V8.8` [35]. The thermodynamic model used is NRTL. This model was developed to represent the phase behaviour of moderately and strongly non-ideal liquid mixtures by taking into account the effects of both differing molecular size and intermolecular forces [36]. Moreover, NRTL is considered as a performing model in process simulation [37].

In the present section, the modelling of the electrolysers used is presented and the two processes are described, step by step. For both cases, a heat integration is considered to optimise the processes.

Proton Exchange Membrane Electrolyser

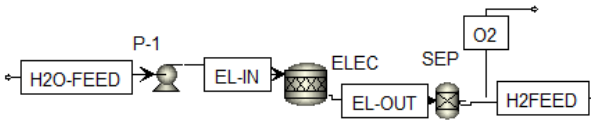

Fig. 1: `Aspen Plus` flowsheet of the PEMEC.

To model the PEMEC, the flowsheet presented in Figure 1 is used. Pure water at EPA standard pressure and temperature, 25°C and 1 atm, enters the process. A pump is used to set the pressure entering the electrolyser where the reaction happens. As the main purpose of this study is not the electrolyser, a mass and energy balance is sufficient. Consequently, the electrolyser is simply modelled as a reactor with a fixed conversion of 100%, even if in reality, a recycling loop of the pure water should be considered.

In `Aspen Plus`, O_2 and H_2 are mixed together and have to be separated. Nevertheless, in reality, the gases are produced in two different compartments and do not need further separation. The purity of both flows is around 100%.

As explained in the cost analysis section below, storage of H_2 needs to be considered too. Both processes are designed to produce H_2 by electrolysis during 18 hours per day only, leading to periods when no electricity from the grid is used for the functioning of the electrolysers. This design is chosen to consider the intrinsic variability of renewable energy sources and it allows to buy cheaper electricity in compensation for grid management services.

Therefore, H_2 reserves have to be made to feed the steady-state processes during periods without electricity consumption. It means that more H_2 is produced than directly consumed and part of this production is stored in large vessels at high pressure. This step is not modelled in `Aspen Plus` as only a storage vessel is required. Nevertheless, its cost is taken into account in the cost analysis.

To avoid a costly gas compression step and as PEMEC can operate under a pressure of 200 bar [31], the entering water is first compressed via a pump at 180 bar before being electrolysed. This early compression allows to decrease the size of the storage vessel for the surplus of H_2 and to produce easily condensed and stored oxygen that can be sold afterward.

Ammonia production

The modelling of the process for the ammonia production is presented in Figure 2. It comprises first the modelling of the PEMEC. The H_2 produced is then mixed with N_2 and the two components react in the reactor R-301. The products are then cooled. Five flash tanks in series are required to obtain the desired purity of ammonia and the vapour phases leaving the first three ones are recycled to the entrance of the reactor as they contain most of the H_2 and N_2 that have not reacted . The heat exchangers network is also designed.

The different parts of the process are detailed in the following sections.

Electrolyser

The electrolysis is modelled in `Aspen Plus` as shown in Figure 1 for a flow rate of pure water of 112 t/h. The amount of electricity required for the electrolyser cell is 12 500 kWh per ton of ammonia produced [9]. The power required for the functioning of a PEMEC being of 700 MW, the electrolysis is performed with 10 to 20 PEM electrolysers in parallel.

Inlet

The plant is sized to produce 540 000 tons per year, *i.e.* 1500 tons per day, of ammonia, according to the average size of an ammonia production site [11].

High-purity liquid N_2 sold in the market at -98°*C* and 180 bar [38] enters the process at a flow rate of 59 tons per hour. It is then vaporised until it reaches at least -20°C. Contrary to the processes that use gas reforming, N_2 has to be pure so air cannot be directly used. A cryogenic distillation of air could be used but the purchase of pure N_2 is considered in this work in order to focus on the ammonia production.

N_2 and H_2 are then mixed together along with the flow of recycled unreacted gases and the mixture is heated before entering the reactor.

Reactor

The reaction (1) is reversible. The kinetics of formation is described in [39], [40] and [41]. Equation (5) expressing the kinetics in a pseudo-homogeneous phase is used as a reasonable approximation for a feasibility study. Numerical parameters k, K_a and α are extracted from Dyson, 1968 [39].

$$r_{NH_3} = 2k\left[K_a^2 a_{N_2}\left(\frac{a_{H_2}^3}{a_{NH_3}^2}\right)^{\alpha} - \left(\frac{a_{NH_3}^2}{a_{H_2}^3}\right)^{1-\alpha}\right] \quad (5)$$

The reaction can be conveyed in a catalytic multi-bed plug flow reactor [42] which consists in several layers of catalytic bed in the same reactor separated by intercooling systems. The approximation of an isothermal reactor is made to limit the number of degrees of freedom of the model. This should theoretically lead to a small overestimation of the conversion at a given volume.

A sensitivity study allows to identify acceptable conditions inside the reactor: a pressure of 180 bar, a temperature of 450°C and a 3:1 H_2/N_2 ratio lead to a thermodynamic equilibrium conversion of 35%, which is acceptable as the conversion in the reactors used in ammonia plants is around 20%. To reach the thermodynamic equilibrium, the reactor has to be very large. As a result, the reactor is sized in order to achieve an outlet conversion of 20%, considering that the value used in industry corresponds to a satisfactory CAPEX/OPEX balance. The downside is that the recycling loop is larger, which results in more loss at the purge, more energy required to preheat the stream at the inlet of the reactor and a more powerful compressor to set the recycling flux pressure back to 180 bar.

Separation

The outlet of the reactor is cooled down from 450°C to 0°C in three steps. Further cooling also comes from gas depressurisation. First, a heat exchanger HTX-1 reduces the temperature

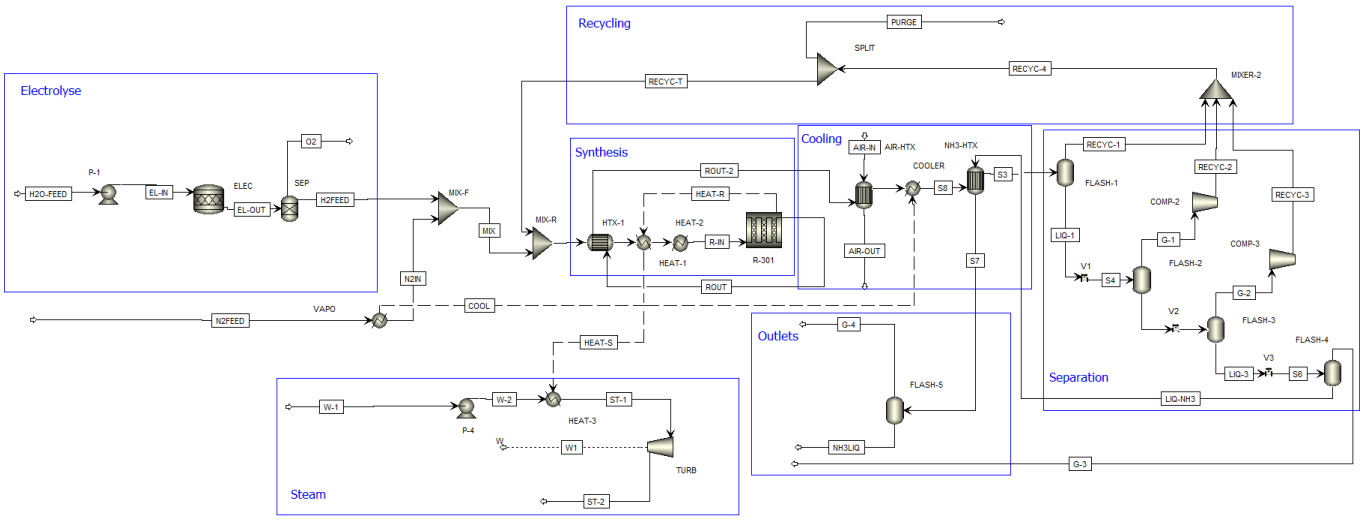

Fig. 2: `Aspen Plus` flowsheet of the ammonia production process.

of the stream to 120°C, then, an air-cooler cools down the hot stream to 40°C and the last cooling step is a heat exchanger with a refrigerant agent.

The separation of ammonia at the outlet of the reactor is achieved using several flash tanks and valves in series, allowing impurities to be removed from the liquid phase. Between each tank, the pressure is reduced via a discharge valve. Four liquid-vapour separations are required, respectively at 180, 50, 10 and 1 bar. This leads to very pure NH_3 in the liquid phase with relatively low presence in the vapour phase. Vapour phases of the first three flash tanks are mixed together to form a recycle loop that is mixed with the pure H_2 and N_2 before their entrance in the reactor. The last flash tank allows to reach a very high purity in NH_3 in the liquid flux NH3LIQ as there is less than 200 ppm of impurities. The vapour stream G-4 is very pure in ammonia too and the vapour flux G-3 has a 93% purity in NH_3. Both are thus valuable products too, as explained in the following section.

Outlets

Three products leave the process: NH3LIQ, G-3 and G-4. Their specifications are presented in Table 1.

Table 1: Specifications of the outlets of the ammonia process, at P= 1 atm.

Properties	G-3	G-4	NH3LIQ
State	vapour	vapour	liquid
Mass flow (t/h)	7,977	41.8	13.5
Temperature ($°C$)	-34.8	-33.4	-33.4
Molar fraction of NH_3	93.1%	1	1
Molar fraction of N_2	6.9%	174 ppm	327 ppb
Molar fraction of H_2	123 ppm	11 ppb	trace

The main product is contained in NH3LIQ. It is the pure ammonia that is sold on the market and can be transported easily as it is in the liquid phase. However, most of the ammonia produced is contained in the vapour phase at 1 atm in G-4. Its storage would thus be costly as a compression chain of 12 MW is needed to store it in a tank of a reasonable size for 24 hours of production. There is another possibility to avoid these additional storage costs: the pure NH_3 can be used directly on site to produce urea, nitrate and other derivatives that could be sold and increase the revenues of the plant [43].

G-3 being less pure, this sub-product can be used to produce nitrate elsewhere in the plant by washing the gas with nitric acid for instance [43], or it could be sold at a cheaper price, but the same storage problem would be encountered.

Many parameters such as the temperature range of each heat exchanger, the number of flash tanks and the pressure in each of them or the purge ratio in the recycling loop could still be optimised to reduce the total cost induced by the equipment size and the energy used by the production process.

Heat Integration

For all the exchanges, a minimum temperature approach difference of 20°C is assumed to limit the size of the heat exchangers. To perform the heat integration, the grand composite curve can be drawn, as presented in Figure 3.

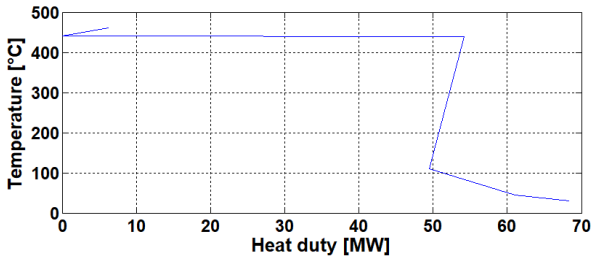

Fig. 3: Grand composite curve of the ammonia process.

It can be seen that the pinch point is at the top limit of the curve, meaning that the process is dominated by hot streams in the whole range of temperature. Consequently, any hot stream may be used to preheat the cold stream at the inlet of the reactor [44].

The outlet of the reactor that must be cooled to 120°C is used to preheat the inlet of the reactor until 331°C. A second part of the preheating is done by using the heat released by the synthesis in the reactor. It allows to reach 430°C, regarding the minimal temperature approach difference. To reach 450°C, an electrical heater is finally used.

The excess of heat generated by the reaction that is not used to preheat the feed allows the generation of high-pressure steam at 100 bar that can be converted into electricity with a turbine, generating 5 MW.

To cool the stream leaving the air cooler from 40°C to 0°C, the N_2 inlet that must be vaporised can be used. However, the maximum energy exchanged only reduces the hot stream temperature to 28°C. To reach 0°C, the liquid ammonia flux leaving the last flash tank at -35°C and 1 bar may be used. With this solution, 75% of the liquid ammonia is vaporised, resulting in two outlets: a very pure gas and a very pure liquid.

It can be concluded that ammonia production via green H_2 is technically feasible without many changes into the synthesis part of the process. The model as presented above also constitutes a basis to estimate the CAPEX and OPEX of the process and allow discussion about the viability of such a project.

Steelmaking

The model of the steelmaking plant is based on a fixed conversion as there is little information on reaction kinetics in the literature. This allows to establish the material and enthalpy balances required to evaluate the feasibility of a steelmaking plant operating with pure H_2. The model built is composed of several units performing different tasks.

The first unit is composed of electrolysers and produces the hydrogen required by the other parts of the process. The second unit is the reacting section, composed of a shaft reactor and different heat exchangers. The iron is reduced in this installation by a direct reduction process. This part of the plant can be considered as the ironmaking step. Another step of the process is the recycling of the H_2 leaving the reactor and its purification by the removal of water, CO and CO_2. The mixture of CO_2, CO and H_2 leaving the process can then be burnt in a fire heater in order to provide energy to some other flows of the process. The last unit of the plant is the EAF, where the iron is melted and refined to produce mild steel. This steel grade is one of the most used and it corresponds to a steel with a carbon content between 0.05% and 0.3%. This process is able to produce 1 000 000 t_{steel}/yr with a carbon content of 0.2%. The global flowsheet modelled in `Aspen Plus` is presented in Figure 4.

Electrolyser

Hydrogen is produced from PEM electrolysers at 80°C under 200 bar. The power consumed by the electrolysers is around 500 MW, allowing the production of enough hydrogen to produce steel continuously and to store a part of it for a further use. The storage tank of H_2 has a minimum capacity of 4000 m^3 in order to store enough hydrogen for 6 hours, which corresponds to around 50 tons of H_2.

DRI process

The reduction of iron is composed of several steps. Each of them can be achieved either with H_2 or with CO. The considered reactions are described below [45].

$$3\,Fe_2O_3 + H_2 \rightarrow 2\,Fe_3O_4 + H_2O \quad (6)$$

$$Fe_3O_4 + H_2 \rightarrow 3\,FeO + H_2O \quad (7)$$

$$FeO + H_2 \rightarrow Fe + H_20 \quad (8)$$

$$3\,Fe_2O_3 + CO \rightarrow 2\,Fe_3O_4 + CO_2 \quad (9)$$

$$Fe_3O_4 + CO \rightarrow 3\,FeO + CO_2 \quad (10)$$

$$FeO + CO \rightarrow Fe + CO_2 \quad (11)$$

The reduction of iron with hydrogen has faster kinetics than the reduction with CO, but reactions (6), (7) and (8) are globally endothermic while reactions (9), (10) and (11) are exothermic [46]. Common DRI technologies, such as *Midrex* and *Energiron*, use a reducing gas composed of a mixture of the two reductants [47, 48].

A plant based on a reduction with only H_2 should be avoided as the reduced iron without any carbon content is very reactive, which can lead to explosion [17]. Therefore, a minimum amount of carbon has to be added in the direct reduction process. It seems thus logical to keep a small injection of CO in the reactor as it can react with FeO to produce Fe_3C following the reaction (12). This additional feed is a 40 kmol/h flow that can contain up to 15 % of CO_2.

$$3\,FeO + 5\,CO \rightarrow Fe_3C + 4\,CO_2 \quad (12)$$

CO can also produce carbon soot according to Boudouard's equilibrium (13). This carbon decreases the reactivity of the reduced iron produced.

$$2\,CO \rightarrow C + CO_2 \quad (13)$$

Most DRI technologies use a shaft reactor where the iron ore is reduced by a counter-current reducing gas mixture. This equipment is divided into three steps: the iron ore is heated to increase the kinetics of the reactions in the upper part of the shaft, the reduction of the ore occurs in the middle part and the bottom of the equipment is used as a reformer and allows the cooling of the DRI. Nevertheless, when the reduction is mainly conducted with H_2, the DRI is already cold as the shaft is an adiabatic reactor and as the reactions (6), (7) and (8) are endothermic. Therefore, there is no need for a reformer and the bottom of the shaft reactor should be replaced.

The design proposed allows to keep the same shape of reactor than common DRI processes. Only the feeds of the shaft have to be changed. The upper part of the shaft is still used to pre-heat the iron ore, its reduction occurs in the middle part and a deeper reduction with CO occurs in the bottom part. With this design, the heat generated by the reactions (11), (12) and (13) is used to keep the upper part at a good temperature. Furthermore, it ensures that CO is mainly consumed by reactions (11), (12) and (13) rather than by reactions (9) and (10).

The optimal temperature of the hydrogen feed is around 850°C. At lower temperatures, the kinetics is slower, which results in an increase of the reactor size. At higher temperature, a sticking phenomenon can be observed [17, 49]. This issue leads to the increase of the size of each particle of iron, which slows down the reaction kinetics due to a longer diffusion time [50]. The CO is fed to the shaft at a temperature of 800°C as reactions (11), (12) and (13) are exothermic and as the sticking phenomenon has to be avoided. This temperature fixes the temperature of the reduced iron leaving the shaft.

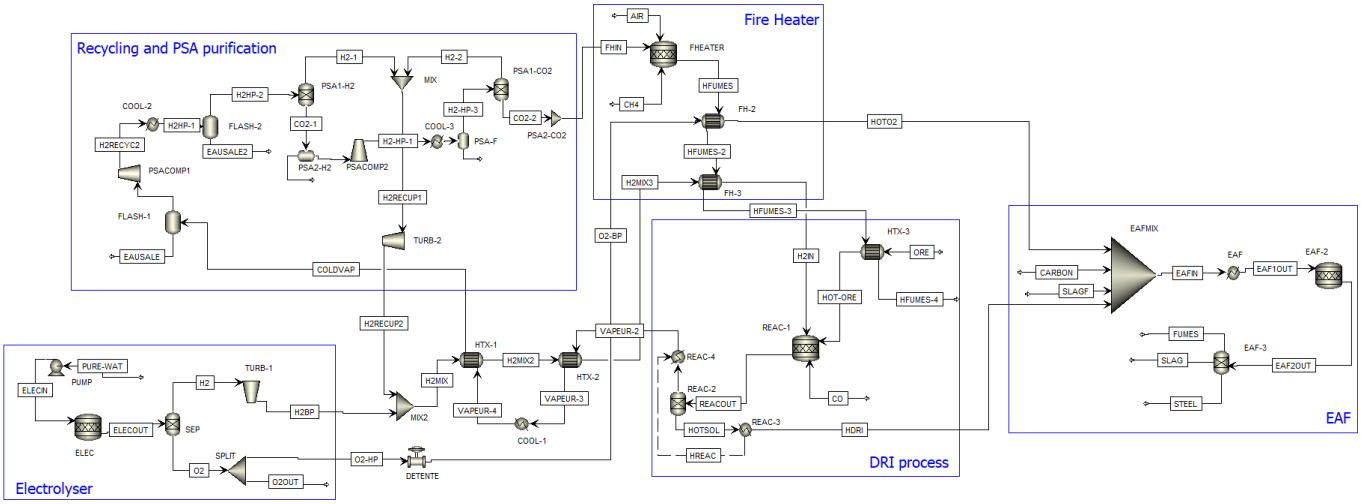

Fig. 4: `Aspen Plus` flowsheet of the steelmaking process.

The main feed composition contains mostly H_2, but a small amount of CO coming from the recycling of the exhaust gas of the shaft is also present. It corresponds to a 11 000 kmol/h flow that includes more than 99 $\%_{mol}$ of H_2.

The stoechiometric ratio of hydrogen required for the complete reduction of iron is 3 $mol_{H_2}/mol_{Fe_2O_3}$. Nevertheless, a higher ratio allows to increase the reaction kinetics and to keep a sufficiently high temperature in the shaft. For those reasons, the ratio could be up to five times the stoechiometric ratio, which corresponds to 15 $mol_{H_2}/mol_{Fe_2O_3}$ [50]. The excess of hydrogen has to be recycled as H_2 is produced from electrolysis at a high cost. However, a part of this H_2 leaves the process with the dirt drain. This amount of lost H_2 is proportional to the hydrogen ratio chosen in the reactor. Therefore, a ratio of 10 $mol_{H_2}/mol_{Fe_2O_3}$ in the ore is chosen. As most of the H_2 is recycled, the hydrogen feed of the plant is around 3 250 kmol/h, which corresponds to 400 $Nm^3_{H_2}/t_{ore}$.

The iron ore feed should be pre-heated in order to increase the kinetics of reaction and avoid energy loss in the shaft. The ore is assumed to contain 95% of Fe_2O_3 and 5% of gangue [50, 51]. A good quality of the ore is important in order to decrease the energy cost related to the impurities. Gangue is mainly composed of SiO_2 and Al_2O_3. The amount of iron ore fed to the shaft is adjusted in order to produce 1 000 000 t_{steel}/yr, which corresponds to the consumption of 181 t_{ore}/h for a plant that operates 8200 h/yr. As standard *Midrex* shafts have a residence time of 6 hours, the volume of the shaft has to be around 150 m^3 [52].

A third flux enters at the bottom of the shaft. It is composed of CO and can come from different sources. A first possibility is to use a waste flux of an external industry. As CO is a toxic gas that cannot be released into the air, it can be interesting for a company to give its undesired by-product rather than building a purification equipment. The required flux of CO can also be produced from partial combustion of organic components.

There are two outlets of the shaft reactor: the DRI and the exhaust gas. The gas can be cleaned and recycled while the DRI, which is at a temperature higher than 600°C, can be transformed into HBI for transport or can be directly fed into an EAF as HDRI.

Recycling loop

The exhaust gas of the shaft contains a non-negligible amount of hydrogen. As the production of this component is one of the major constraints for the modelling of the plant, H_2 has to be recycled. Nevertheless, the outlet stream is also contaminated with water, CO_2 and CO. Therefore, a purification process has to be included inside the recycling loop.

The first step is the removal of water from the gas. It can easily be performed by cooling the stream to a temperature around 5°C. At this temperature, water condenses while other components are still in the vapour phase. A flash tank can thus be used to separate the two phases. An important remark is that the flash tank cannot be at 0°C or at a lower temperature. Indeed, as the liquid phase contains nearly pure water, it would freeze, which would damage the equipment and force the shut down of the plant. There is still a small amount of water in the vapour phase leaving the flash tank. Therefore, additional flash tanks are added after each cooling step in the purification process.

The vapour phase stream contains mostly hydrogen, but small amounts of water, CO_2 and CO are also present in the flux. CO can be recycled as it can reduce iron ore, but CO_2 and water have to be removed or they would never leave the system. This issue can be solved with the use of a two-stage pressure swing adsorption (PSA) [53, 54]. The first stage is used to recover pure H_2 but this stream contains only 90% of the initial amount of H_2. A second stage is thus needed and allows a recovery of around 99% of the amount of H_2 present in the exhaust gas of the shaft. However, the second PSA does not produce pure H_2. The top stream is also composed of CO and a very small amount of CO_2.

Both PSA stages operate at a pressure of 7 bar for the selective adsorption of impurities and the regeneration takes place at a pressure of 0.1 bar [53]. The outlet streams of the two-stage PSA, containing mainly H_2, can be recycled to the shaft, while the remaining mixture of CO_2, CO and H_2 is purged. As this purge stream contains around 100 $kmol_{H_2}$/h, it can be valued by burning it in a fire heater. This fire heater is also fed with CH_4 and O_2 in order to produce enough heat to pre-heat the

inlet of the shaft reactor and other small fluxes.

Electric arc furnace

The EAF is fed with HDRI, carbon and slag former. Scrap could also be charged instead of a part of the DRI. The carbon source shall contain as few volatile compounds as possible in order to avoid excessive energy consumption due to their combustion. The slag former is generally composed of limestone but it can also be composed of dolomite.

Once the bucket is fully charged, the mixture it contains is melted. If the volume of the melt is much lower than the volume of the solid mixture, the bucket can follow a second step of charging and melting. It is the case when a high amount of scrap is fed into the EAF.

The temperature of the melt is set around 1 650°C [24, 25]. The energy required is provided by chemical reactions and by the electric arc generated by the EAF. Chemical energy is either provided by slag formation or slag foaming. The slag is composed of CaO, Al_2O_3, SiO_2 and FeO. Oxygen is fed to the EAF to provide energy and to allow slag foaming. The foaming phenomenon is due to the reactions (14), (15) and (16) [25, 51, 55].

$$\mathrm{FeO} + \mathrm{C} \rightarrow \mathrm{Fe} + \mathrm{CO} \tag{14}$$

$$\mathrm{C} + \frac{1}{2}\,\mathrm{O_2} \rightarrow \mathrm{CO} \tag{15}$$

$$\mathrm{C} + \mathrm{O_2} \rightarrow \mathrm{CO_2} \tag{16}$$

The slag also allows to refine the iron phase by absorbing most of the impurities. At the end of the refining stage, the liquid steel can be fed to continuous casting. This step allows the transformation of hot liquid steel into usable solid steel. It is not modelled with `Aspen Plus` as this process is the same for all kind of steelmaking and complete equipment can directly be bought on the market [56, 57, 58].

At the end of the process, 135 kg of slag are generated for each ton of steel produced. As the slag solidifies at high temperature, the energy it contains cannot be recovered.

Around 30 Nm^3 of oxygen are injected in the EAF per ton of steel, so the same amount of gas leaves it. This exhaust gas contains CO, CO_2 and O_2. A post-combustion of those gases is interesting in order to generate heat to pre-heat the inlet of the next bucket of the EAF. However, those fumes have to be cooled quickly and it is difficult to use them for heat integration [17]. Furthermore, the exhaust gas of the EAF contains a lot of dust. It is estimated that around 15 kg of dust have to be removed from the gas for each ton of steel produced [59].

Heat integration

Steelmaking is an energy intensive process, especially when the iron reduction is made with H_2. Integrating as much as possible the process allows to decrease the energy consumption of the plant.

The grand composite curve of the process is presented in Figure 5. This curve is built with a minimum temperature approach difference of 20°C. It can be seen from this graph that the process requires at least two utilities. The ideal hot utility should provide 46 MW while the cold utility should remove 34 MW of heat. Those values are quite huge as the process requires energy at high temperature and the heat removed from the system is at low temperature.

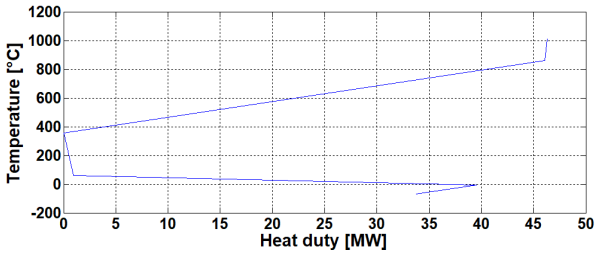

Fig. 5: Grand composite curve of the steelmaking process.

The bottom part of the grand composite curve shows that the outlet flow of the reactor should pre-heat the feed of the shaft. The cold utility is used to finish the cooling of the exhaust gas of the reactor and river water could be used for this purpose for instance.

A hot utility is also required by the system as the feed of the reactor has to be heated up to 850°C while there is no other stream at this temperature in the process. A small amount of oxygen has also to be heated before entering the EAF. Both flows can be heated with the use of a fire heater. This equipment is fed with a mixture of H_2 and CH_4. The source of H_2 is the recycling of the soiled gas of the purification. Indeed, this stream contains H_2 and CO that can be burnt.

The fumes generated by the fire heater still contain energy after having heated the feed of the shaft. This excess heat is recovered by pre-heating the iron ore before its injection in the reactor.

COST ANALYSIS

Formulas extracted from Turton et al. [60] and from Nilsson et al. [61] are used to calculate CAPEX, OPEX and cash flows. All the costs in this section are estimated for the year 2030. Consequently, these costs are rounded to be presented in a more visual way.

Proton Exchange Membrane Electrolyser

The cost of a PEMEC, without its installation is currently of 700 €/kW and it is expected to decrease to 500 €/kW by 2030 [9]. The electrolysis is the most electricity-consuming step of both processes. Given the large required amounts of H_2, many PEMEC are needed. The cost of electricity is thus an important factor for the viability of the processes.

The cost of electricity in Europe is assumed to be 40 €/MWh for both processes. Indeed, it can be seen in Figure 6 that for the ammonia production, a classical plant consumes less than 100 GWh/yr at a price of 70 €/MWh but, as a low-carbon emission plant of a classical size consumes around 5 000 GWh/yr, the price of the electricity decreases [62]. The inverse proportionality between the electricity consumption and its price leads to a mean price of 40 €/MWh for the important electricity consumption of the low-carbon emission plant. The same price is used for the steelmaking process.

Even with this reduced price of electricity, the impact of the electricity consumption on the total costs of the processes

can be understood. For instance, the capacity required for the desired production of ammonia is 700 MW, inducing an operating cost of more than 250 million €/yr if the cost of electricity is 40 €/MWh. The electricity consumption is thus one of the most important factors for the total cost of the process.

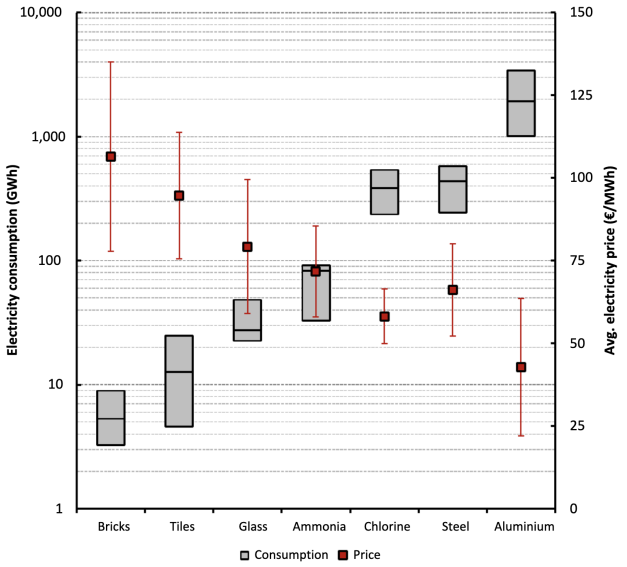

Fig. 6: Correlation between the electricity price and the electricity consumption for common plants of different sectors [62].

In order to decrease these huge operating costs, a peak shaving approach can be considered. Peak shaving consists in stopping the electricity consumption of the plant during parts of the day when consumption peaks occur on the electrical grid, in order to help the electricity supplier to cope with peaks of demand from other consumers. Those peaks occur because the demand for electricity varies during the day, depending on whether people are at work or at home, and because the grid is assumed to be partially provided by renewable energies so the offer will also fluctuate depending on the weather conditions. If a process is able to operate without or at least with less electricity from the grid during some periods of the day, better prices can be negotiated with the electricity supplier. From the possibility to operate without electricity, a decrease by 25 to 35% can be expected [63], leading to a cost of maximum 30 €/MWh. The processes are designed to consider a peak shaving of 6 hours per day, spread throughout the day. To operate without electricity for the electrolysers, H_2 has to be stored during the 18-hour period when electricity is supplied in order to be available for the 6-hour period left when the electrolysers are at a standstill. The rate of H_2 production by the electrolysers increases thus by 33% as the same amount of H_2 has to be produced during a smaller period. To cope with this rise, the number of electrolysers is increased. In the ammonia plant for instance, the capacity increases from 700 to 900 MW, so between 10 and 20 electrolysers are required. 75 ton of H_2 have to be stored each day. H_2 is stored as a gas as it is already at 180 bar when it is produced by the electrolyser. A 6000 m^3 tank is sufficient to store it.

The same system is applied for the steelmaking plant. Nevertheless, only 50 tons of H_2 have to be stored each day. Therefore, only a 4000 m^3 tank is required for its storage.

Ammonia production

The costs of the different equipment are estimated for 2030 with the Turton [60], using an interpolation of the values of the Chemical Engineering's Plant Cost Index, CEPCI, from previous years. The CEPCI value for 2030 is estimated at 750 [64, 65].

The choice of a normal size plant producing 1500 t_{NH_3}/day is made. Such a size allows to benefit from the economy of scale. Indeed, the larger the plant, the easier the possibility of purchasing raw materials at a lower per-unit price. Moreover, the plant is not too large as it would be difficult to supply it with green electricity and as the number of equipment would have to be doubled because their size cannot increase indefinitely. Some important costs of the ammonia production process are listed in Table 2 below.

Table 2: Main equipment costs for the ammonia process in 2030.

Equipment	Number	Characteristic value	Unit Cost (€)
FLASH-1	1	18 m^3	2 115 000
FLASH-2	1	17.8 m^3	2 000 000
FLASH-3	1	14.8 m^3	1 700 000
FLASH-4	1	14 m^3	1 600 000
FLASH-5	1	17 m^3	2 500 000
R-301	1	35 m^3	15 000 000
COMP-1	1	141 kW	260 000
COMP-2	1	721 kW	1 000 000
COMP-3	3	3000 kW	2 850 000
P-1	1	300 kW	350 000
P-2	1	300 kW	350 000
P-3	1	200 kW	260 000
P-4	1	126 kW	180 000
HTX-1	1	1250 m^2	1 000 000
NH3-HTX	1	433 m^2	350 000
Air-1	1	1917 m^2	1 000 000
ELEC	20	45 MW	25 000 000

From the costs of the equipment in Table 2, the total grassroots plant cost is estimated at 800 000 000 €. This value also takes into account auxiliary facilities and the purchase of the land in case of a new plant [66].

In terms of OPEX, the costs are estimated from different sources for the prices of the raw materials [12, 67, 68]. The costs of the raw materials needed in the plant are listed in Table 3 and those of the products are listed in Table 4.

Table 3: Raw materials costs for the ammonia process in 2030.

	Cost (€/t)	Flow rate (t/yr)	Cost (€/yr)
Nitrogen	30	478 880	14 366 400
Pure water	1	911 020	911 020

Table 4: Products costs for the ammonia process in 2030.

	Cost (€/t)	Flow rate (t/yr)	Cost (€/yr)
Oxygen	27	809 102	21 845 759
Ammonia	350	512 500	179 375 000

The price of methane also has an important impact on the price of ammonia. If it drops, the income value will also decrease, making the plant less profitable. This correlation is represented in Figure 7 for the prices of ammonia and methane in the US [69].

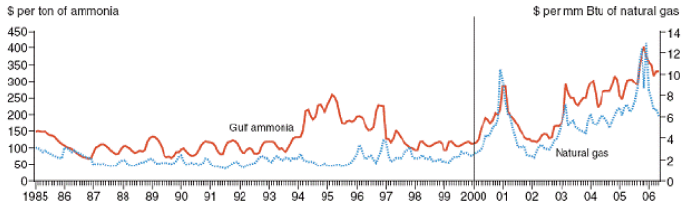

Fig. 7: Evolution of the US prices of natural gas and ammonia [69].

Regarding Figure 7, it is clear that the ammonia price follows the methane price. The same correlation can be transposed to Europe. Owning an ammonia plant from green hydrogen makes the price of the produced ammonia independent from the methane cost. In case of an increase of the methane price, the low-carbon emission plant will become more profitable as a classical plant has a share of natural gas in its total production costs of 80 to 88% [70]. Nevertheless, no valid cost estimation on the evolution of methane can be made as its price is influenced by geopolitical conflicts and industrial lobbying. Therefore, no change in the estimated cost of methane can be considered viable.

The number of ammonia plants that will switch to low-carbon emission plants will also influence the importance of this correlation. Indeed, if most of the ammonia production plants follow the decarbonisation trend, the influence of the price of methane on the price of ammonia will decrease and the cost of electricity will become more impacting.

Concerning the labour cost, a salary of 25 €/h is considered with six working positions. The labour cost value is estimated at 1 500 000 €/yr.

As mentioned in the previous section, the price of electricity has an important impact on the income revenue of the plant. This cost can be negotiated with the peak shaving approach explained previously.

Another important point in 2030 for ammonia plants in Europe will be the cost of the CO_2 emissions. Currently, European companies that emit CO_2 have to buy emission allowances to be legally authorised to emit CO_2, otherwise heavy fines are imposed [71]. The price of those allowances depends on the market price, a company being allowed to buy excess allowances from another company. At the end of 2019, the allowances cost was around 25 €/t_{CO_2} [72]. In the coming years, the cost of the CO_2 emissions is expected to increase and other forms of taxes could be imposed. Estimations show that this cost should reach 50 €/t_{CO_2} to 100 €/t_{CO_2} by 2030 [73]. The cost of the CO_2 in 2030 is thus assumed to be of 75 €/t_{CO_2} in the present work. The increase of this cost will have a direct impact on the ammonia production costs in Europe for ammonia plants that use natural gas reforming. This will lead to an increased interest in low-carbon emission plants.

The discounted cash-flow diagram of the process for a lifetime of 30 years is presented in Figure 8. The inflation rate used for the study is 1.5%. The discounted rate, *i.e.* the return on investment desired each year, is approximated at 10% and the depreciation period is fixed at 10 years.

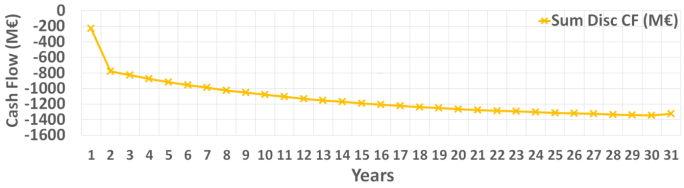

Fig. 8: Discounted cash flow diagram of the ammonia production in the base case.

Figure 8 shows that a green ammonia plant, in these conditions, is not economically viable.

Some parameters have thus to vary to be able to design a profitable process. The price of electricity is a first parameter. The evolution of the income revenue of the plant as a function of the electricity price is presented in Table 5.

Table 5: Income revenue of the ammonia production process for different electricity prices, with a cost of CO_2 emission of 75 €/t_{CO_2}.

Electricity price (€/MWh)	Income revenue (€/yr)
30	-109 500 000
25	-77 500 000
20	-45 500 000
15	-13 500 000
13	-500 000
10	19 000 000
5	51 000 000

It can be seen in Table 5 that, for a cost of the CO_2 emissions of 75 €/t_{CO_2}, the income revenue becomes positive only for a price of electricity lower than 13 €/MWh. With these values, even if the income is positive, the discounted cash flow still stays negative after 30 years. Figure 9 shows the evolution in these conditions.

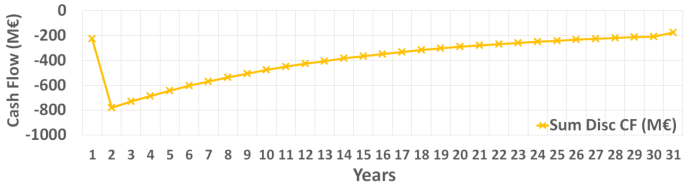

Fig. 9: Discounted cash flow diagram of the ammonia production for an emission cost of 75 €/t_{CO_2} and an electricity price of 12 €/MWh.

The cost of the CO_2 emissions is a second influencing factor. A sensitivity analysis on this cost and on the price of electricity is presented in Figure 10, for the discounted cash flow.

Figure 10 shows that, in order to obtain a positive discounted cash flow after 30 years and thus design a viable process, some

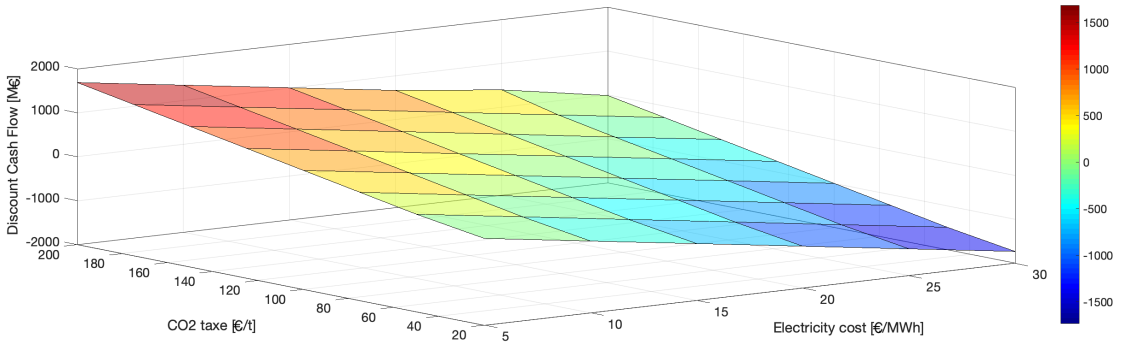

Fig. 10: Sensitivity analysis on the price of electricity and on the cost of CO_2 emissions for the discounted cash flow of the ammonia process after 30 years.

modifications in the costs have to be considered. Depending on the cost of electricity and with the assumed interest and index rates, a minimum value for the cost of the CO_2 emissions has to be set to obtain an economically viable process. These minimum values are listed in Table 6 for different electricity prices.

Table 6: Minimum amounts of the CO_2 emissions cost to design a viable process after 30 years, for different electricity prices.

Electricity price (€/MWh)	Minimum CO_2 cost (€/t_{CO_2})
30	220
25	185
20	150
15	115
10	80
5	46

The needed subventions to build a profitable low-carbon emission plant compared to a classical plant can be calculated from the electricity required to make one ton of ammonia from green hydrogen and from the cost of the CO_2 emission related to one ton of ammonia produced by gas reforming at a price of 350 €/t_{NH_3}. If the price of the electricity is 30 €/MWh, 396 €/t_{NH_3} of subsidies are required to be profitable. These 396 €/t_{NH_3} can result from an increase of the CO_2 cost or from a decrease of the price of electricity. An increase in the CO_2 cost would directly impact the price of ammonia from gas reforming as 1.8 tons of CO_2 are emitted per ton of ammonia produced [4]. Similarly, the electricity price influences the cost of the ammonia produced as 12.5 MWh of electricity are required to produce one ton of ammonia with pure H_2 from electrolysis [4].

The cost of ammonia can also increase, reducing the needs for subventions, but the present work only studies the worst case, with a cost of 350 €/t_{NH_3}.

Conducting a sensitivity analysis on the cost of the CO_2 emission up to 200 €/t_{CO_2} is not that utopian. Indeed, the Dutch government is currently approving a climate law that intends to introduce a CO_2 flat tax from 2021 that will increase up to 150 €/t_{CO_2} by 2030 [68, 74], in addition to the European allowances. However, as ammonia is a commodity, there is a global ammonia market price. Therefore, such CO_2 prices have to be internationally accepted or Europe has to establish carbon import taxes in order to protect the industry from the risk of so-called carbon leakage, the shift of the production outside of the regions with carbon pricing.

Steelmaking

The costs of the different equipment are estimated for 2030 in Table 7 [60, 61], using the interpolation of the value of the CEPCI for 2030, as done for the cost evaluation of the ammonia production process [64, 65].

Table 7: Main equipment costs for the steelmaking process in 2030.

Equipment	Number	Characteristic value	Unit Cost (€)
REAC	1	1 000 000 t/yr	286 000 000
EAF	1	1 000 000 t/yr	240 000 000
HTX1	1	875 m^2	750 000
HTX2	5	1000 m^2	870 000
HTX3	1	116 m^2	170 000
COOL-1	3	775 m^2	670 000
COOL-2	1	435 m^2	400 000
COOL-3	1	55 m^2	130 000
VESSEL	1	4 000 m^3	3 800 000
FHEATER	1	50 MW	13 750 000
PSA	2	/	11 730 000
ELEC	9	45 MW	25 000 000
TURB1	1	6.4 MW	4 500 000

In Table 7, the compressors and associated coolers are included in the price of the PSA units. To the total cost of equipment for CAPEX, the price of the casting stage that has not been modelled in `Aspen Plus` has to be added. This is estimated at a cost of 273 million € in terms of grassroots plant cost in 2030 [58, 75]. The total grassroots plant cost can be estimated at 1 560 000 000 € from the costs of the equipment presented in Table 7 and the cost of the casting of steel [66].

For the OPEX, the costs are estimated from different sources for the prices of the raw materials [68, 76, 77, 78, 79, 80, 81, 82]. The costs of the raw materials required by the process are listed in Table 8. To these costs are added the costs of casting, which are estimated at 100 €/t_{steel}. The total annual costs for this process step are therefore 100 000 000 €. The costs of the products sold are

also displayed in Table 9. It is important to note that the selling price of steel fluctuates significantly over time, so a sensitivity analysis on this price is performed later in this work. The price of steel considered in Table 9 is the price of August 2019.

Table 8: Raw materials costs for the steelmaking process.

	Cost (€/t)	Flow rate (t/yr)	Cost (€/yr)
Hematite	45	1 485 168	67 000 000
Pure water	1	480 151	480 000
Anthracite	400	18 409	7 400 000
Lime	63	66 493	4 200 000
CH_4	220	27 855	6 100 000

Table 9: Products costs for the steelmaking process.

	Cost (€/t)	Flow rate (t/yr)	Cost (€/yr)
Steel	540	1 000 000	540 000 000
Oxygen	27	472 369	12 750 000
Slag	5	136 161	680 000

Concerning the labour cost, a salary of 25 €/h is considered with six working positions, resulting in a labour cost value estimated at 2 800 000 €/yr.

As mentioned in the cost analysis of the ammonia process, the price of electricity has an important impact on the income revenue of the plant. This cost can be negotiated with the peak shaving approach. Values of the income revenue are listed in Table 10 as a function of the price of electricity.

Table 10: Income revenue of the steelmaking process for different electricity prices, with a price of steel of 540 €/t_{steel}.

Electricity price (€/MWh)	Income revenue (€/yr)
30	-26 700 000
25	- 13 400 000
20	- 100 000
19	2 500 000
15	13 200 000
10	26 500 000
5	39 800 000

It can be seen in Table 10 that the price of electricity has a significant impact on the income revenue of the plant. Indeed, the income revenue becomes positive only for a price of electricity of 19 €/MWh. The evolution of the cost of the CO_2 emissions in the next years is not taken into account in this calculation. However, it is obvious that the more the cost of the CO_2 emissions will increase, the more beneficial it will be for the decarbonised plants. These revenues are estimated for the year 2030 with assumptions such as lower PEMEC prices and lower electricity costs due to peak shaving.

In Figure 11, the obtained discounted cash flow diagram for a lifetime of 30 years is displayed. The electricity price considered is 30 €/MWh. The inflation rate taken into account for the study is 1.5%. The discounted rate is approximated at 10% and the depreciation period is fixed at 10 years.

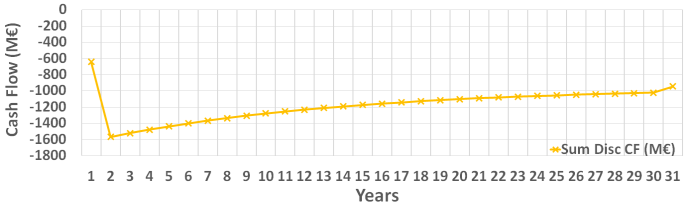

Fig. 11: Discounted cash flow diagram of the steelmaking process in the base case with a price of steel of 540 €/t_{steel}.

Figure 11 shows that a low-CO_2 emission steelmaking process is not economically viable for a price of electricity of 30 €/MWh. Indeed, the discounted cash flow is never positive in this case. That means that the investors will have a negative rate on their investments even after 30 years.

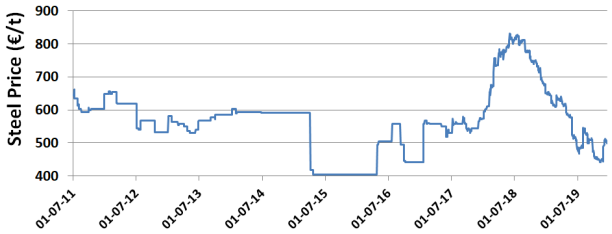

Fig. 12: Exchange rate of steel between 2011 and 2019.

As can be seen on Figure 12, price of steel has varied widely during the previous years [79, 80]. Therefore, a sensitivity analysis of the plant's revenue based on this price is relevant.

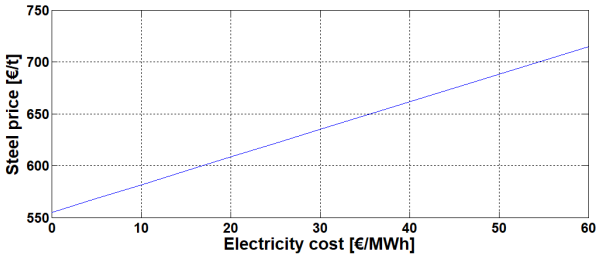

Fig. 13: Limit of profitability of the steelmaking process after 30 years.

Figure 13 shows the conditions to obtain a positive discounted cash flow diagram after 30 years and thus design a viable process: the plant is only economically viable above the curve. For instance, it can be seen that for a price of electricity of 30 €/MWh, the limit of profitability is reached for a steel price corresponding to approximately 635 €/t.

As the price of steel reached more than 840 €/t in 2018, the analysis below is based on this price [79, 80]. Table 11 presents the income revenue as a function of the electricity price in the case of a high price of steel.

Table 11: Income revenue of the steelmaking process for different electricity prices, with a price of steel of 840 €/t_{steel}.

Electricity price (€/MWh)	Income revenue (€/yr)
30	273 000 000
20	300 000 000
10	326 600 000

Table 11 can be compared with Table 10. The huge differences between two corresponding values of these two tables highlights the fact that the plant's revenues are extremely dependent on the price of the steel. Nevertheless, the price of the steel in August 2019 that is considered in Table 10 was almost at its lowest value in more than 10 years. The risk of the price falling further is therefore rather limited. In fact, the trend of the last months of 2019 shows an increase in the price of the steel [79]. In addition, as explained before, negotiations on the price of electricity can also lead to an important decrease of the OPEX. Benefits can also be obtained through the reduction of CO_2 emissions.

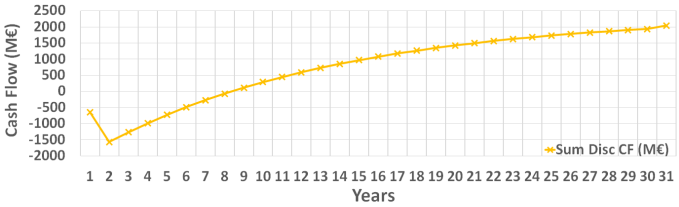

Fig. 14: Discounted cash flow diagram of the steelmaking process for a high price of the steel of 840 €/t_{steel}.

Figure 14 shows that the low-CO_2 emission steelmaking process designed in the present article could be economically profitable in the case of the high price of the steel of 2018, even with a price of electricity of 30 €/MWh.

The cost analysis of the steelmaking plant highlights the fact that the viability of the process is very dependent on the price of electricity and steel. Furthermore, the total investment cost is huge and it may be difficult to attract investors. Nevertheless, if it is possible to make contract with electricity suppliers to decrease as much as possible the electricity cost and if the price of the steel does not crash, this kind of low-carbon emission plants could be built in a near future.

Conclusions

In this work, two industrial processes are studied, regarding the feasibility of a transition to low-carbon emission plants. First a literature review summarises the current processes and state of the art technologies for different types of electrolysers for the production of H_2. The modelling on `Aspen Plus` of both processes and of the proton exchange membrane electrolyser is then detailed. The cost analyses of the two processes are then conducted to evaluate the feasibility of the envisaged transition, regarding different scenarios for the evolution of the main factors. This study showed that, to reach the objective of a viable decarbonised industry, many assumptions on the developments of technologies and on the political and economic decisions have to be made.

First, PEMEC, or other performing electrolysis technologies, have to be expanded to the industrial scale. No large-scale PEMEC is used today and the technology has to reach maturity before it can be used in large industries such as those presented in this article.

Based on already existing production processes, the transition to decarbonised processes can be envisaged. The processes have to be adapted to use pure H_2 produced by electrolysis as raw material. This transition should be easy to implement for the ammonia production as pure H_2 is already used, thus only the gas reforming step should be replaced by the production of H_2 with electrolysers in theory.

The modification of the steelmaking process would require more reflection as most of the production sites are designed to operate with a CO-H_2 mixture as reducing agent. The transition to pure H_2 requires thus deep studies to modify the operating conditions in the process.

Another factor that will influence the feasibility of the studied transition is the cost of electricity. Indeed, for both processes, the electricity consumption is the major cost of the process so its price will strongly influence the revenues. Depending on the negotiations with the electricity suppliers and the possibility to cope with peak shaving, reduction of the prices can lead to important modifications of the income revenues.

Political decisions will also decide whether transition to decarbonised industries will take place or not. Indeed, if the European Union takes the measures discussed previously to increase the cost of the CO_2 emissions or tax those emissions and to subsidise the low-carbon technologies, the processes detailed in this article will become really attractive.

Another important subvention channel that is not taken into account in this work is the new investment program from the European Commission. Indeed, the Commission announced an investment programme worth over 10 billion € for low-carbon technologies in several sectors to boost their global competitiveness and the first call for application will be launched in 2020 [68, 83]. These funds intend to promote the transition to decarbonised industries by subsidising part of the investments made to reach that goal. The European Union intends to allocate 60% of the difference between the CAPEX of a classical plant and the CAPEX of the low-carbon emitting one to encourage the companies to decrease their CO_2 emissions. 60% of the difference between the OPEX of the two plants will also be subsidised during the first 10 years of functioning.

Other factors will influence the feasibility of the processes. For instance, the price of the products will play a key role in the development of those less-emitting processes. Rises of the costs of NH_3 and steel would lead to more profit and thus attract new investors.

This work also considers that the electricity will be provided by renewable energies in 2030. Even if the role played by renewable energies in the production of electricity increases each year, it is an important assumption as the share of the renewable energies is not yet expanded in many European countries. The two decarbonised processes operating nearly exclusively with electricity, its production means will thus play

an essential role in the green characteristic of the processes. It is also important that this huge amount of green electricity is easily supplied to the plant. This means probably that either the plant needs to be located near the electricity generation, such as offshore wind farms, or that significant investments in the electricity grid are needed.

Regarding all the aspects developed in this article, criteria for the choice of the plants' location can be determined. Several factors have to be taken into account. First, the accessibility is important. The import of raw materials and export of final products have to be as easy as possible. Locations near harbours or railways should thus be considered. Then the plant should be located in a country with cheap electricity, as it is the most expensive part of the cost. The host land must also produce sufficient green energy to supply the process.

The development of decarbonised processes depends thus on many factors. If enough electricity can be produced by renewable energies and if leaders of governments and chemical industries decide to promote decarbonisation of the large production sites, investments could be allocated to the development of improved processes and new technologies that would lead to huge pollution decreases. Work of many different parties will thus be needed to reach the objective of decarbonised industries, and studies and student contests as the present one should help in the process, being a first step that intends to prove the feasibility of such decarbonised processes.

ACKNOWLEDGEMENTS

The authors would like to thank Prof. G. Leonard for his advice and support through the realisation of the project. Thanks are also addressed to Mr. A. Hoxha and Mr. J. Jouet for having given their time and provided valuable information.

REFERENCES

[1] European environment agency. Final energy consumption by sector and fuel. https://www.eea.europa.eu/data-and-maps/indicators/final-energy-consumption-by-sector-9 / assessment-4, accessed on December 17, 2019.

[2] European environment agency. Greenhouse gas emissions by aggregated sector. https://www.eea.europa.eu/data-and-maps/daviz/ghg-emissions-by-aggregated-sector-5 # tab-dashboard-02, accessed on December 10, 2019.

[3] European Commission. *Rapport de la commission : Quatrième rapport sur l'état de l'union de l'énergie*, 2019.

[4] F. Dolci. Green hydrogen opportunities in selected industrial processes. In *JRC technical reports*, 2018.

[5] Uliege Chemeng. Presentation of eurecha. https://www.chemeng.uliege.be/cms/c_3486141/fr/chemical-engineering-eurecha, accessed on November 4, 2019.

[6] Jayant Modak. Haber process for ammonia synthesis. *Resonance*, 7:69–77, 09 2002.

[7] B. Dabir A. Edrisi, Z. Mansoori. Using three chemical looping reactors in ammonia production process - A novel plant configuration for a green production. *international journal of hydrogen energy* , 39:8271–8282, 2014.

[8] A. Senyshyn M. Behrens R. Schlögl T. Kandemir, Manfred E. Schuster. The Haber–Bosch Process Revisited: On the Real Structure and Stability of "Ammonia Iron" under Working Conditions. *Angewandte Chemie, International edition*, 52:12723–1276, 2013.

[9] F. Ausfelder A.M. Bazanella. *Low carbon energy and feedstock for the European chemical industry*. Dechema, 2017.

[10] L. E. Apodaca. Mineral commodity summaries. In *U.S. Geological Survey*, 2019.

[11] E. van Nieuwenhuyser. *Production of ammonium nitrate and calcium ammonium nitrate*. EFMA, 2000.

[12] Yara. Yara fertilizer industry handbook. 2017.

[13] F. Weins. Who produces the most ammonia in europe? https://www.eurocheddar.com/news-in-europe/who-produces-the-most-ammonia-in-europe, accessed on December 12, 2019.

[14] A.BELLIL. *Optimisation d'un réacteur de production de l'ammoniaque*. PhD thesis, Université Mohamed Khider–Biskra, June 2015.

[15] Zonebourse. Acier : la production mondiale en hausse de 5,3% en 2017. https://www.zonebourse.com/actualite-bourse/Acier-la-production-mondiale-en-hausse-de-5-3-en-2017-\-25864293/, accessed on December 12, 2019.

[16] MIDREX. World direct reduction statistics. , page 16, 2017.

[17] Informal discussion with J. Jouet, Group Chief Technology Officer. John Cockerill, December 17, 2019.

[18] S. W. Haider D. V. Morse H. S. Lee, S. S. Murthy. Primary production scheduling at steelmaking industries. *International Business Machines Corporation*, 40:231–252, 1996.

[19] R. Anantharaman M. Voldsund, K. Jordal. Hydrogen production with CO2 capture. *International journal of hydrogen energy*, 41:4969–4992, 2016.

[20] M. Machida K. Eguchi H. Arai M. Chai, Y. Yamashita. Preparation and characterization of metal-dispersed alumina membranes for selective separation of hydrogen . *Journal of membrane science* , 97:199–207, 1994.

[21] F. Hauler W. A. Meulenberg H.Buchkremer T. Van Gestel, D. Sebold. Potentialities of microporous membranes for H2/CO2 separation in future fossil fuel power plants: Evaluation of SiO2, ZrO2,Y2O3–ZrO2 and TiO2–ZrO2sol–gel membranes. *Journal of membrane science*, 359:64–79, 2010.

[22] M. Jung J. Park, T. Hong. Hydrogen permeation on Al2O3-based nickel/cobalt composite membranes. *international journal of hydrogen energy* , 35:12976–12980, 2010.

[23] M. Burgard B. Ernst, S. Haag. Permselectivity of a nickel/ceramic composite membrane at elevated temperatures: A new prospect in hydrogen separation? *Journal of membrane science* , 288:208–217, 2006.

[24] G. O. Bolarinwa O. O. Biodun S.C.Aduloju, W. S. Ebhota. Process Modeling of Steel refining in Electric Arc Furnace (EAF) for Optimum Performance and Waste Reduction. *Chemical and Process Engineering Research*, 28:13, 2014.

[25] A.M. Fathy G.M. Megahed I. El-Mahallawi H. Ahmed M.M. Elkoumy, M. El-Anwar. Simulation of EAF refining stage. *Ain Shams Engineering Journal*, 9:2781–2783, 2017.

[26] Y. de Lassat de Pressigny M. Schneider-M. Jeanneau J.P. Birat, J.P. Vizioz. Co2 emissions and the steel industry's available responses to the greenhouse effect. *Revue de Métallurgie*, 96, 10 1999.

[27] I. Staffell A. Hawkes J. Nelson S. Few O. Schmidt, A. Gambhir. Future cost and performance of water electrolysis: an expert elicitation study. *International journal of hydrogen energy*, 42:30470–30492, 2017.

[28] H. K. Ho S. C. Tan M. Li. G. Li J. Li Z. Feng X. Zhang, S. H. Chan. Towards a smart energy network: the roles of fuel/electrolysis cells and technological perspectives. *International journal of hydrogen energy*, 40:6866–6919, 2015.

[29] L. Cronin G. Chisholm. *Hydrogen From Water Electrolysis*, chapter , pages 315–343. School of Chemistry, University of Glasgow, Glasgow, 2016.

[30] Production d'hydrogène par électrolyse de l'eau. *AFHYPAC*, page 12, 2017.

[31] I. Staffell A. Hawkes J. Nelson S. Few O. Schmidt, A. Gambhir. Future cost and performance of water electrolysis: An expert elicitation study . *International journal of hydrogen energy*, 42:30470–30492, 2017.

[32] F. Barbir. PEM electrolysis for production of hydrogen from renewable energy sources. *International journal of hydrogen energy*, 78:661–669, 2005.

[33] R. Subrayan S. Wun Cha A. Pandiyan, A. Uthayakumar. Review of solid oxide electrolysis cells: a clean energy strategy for hydrogen generation. *Nanomaterials and Energy*, 8:1–22, 2019.

[34] Informal discussion with N. Job, Associate Professor. University of Liège, December 1, 2019.

[35] Aspentech. Aspen plus. https://www.aspentech.com/products/engineering/aspen-plus, accessed on November 19, 2019.

[36] J.M Prausnitz H.Renon. Local compositions in thermodynamic excess functions for liquid mixtures. *AIChE Journal*, 14:135–144, 1968.

[37] V.Athès M.Esteban-Decloux C.Puentes, X. Joulia. Review and Thermodynamic Modeling with NRTL Model of Vapor–Liquid Equilibria (VLE) of Aroma Compounds Highly Diluted in Ethanol–Water Mixtures at 101.3 KPa. *Industrial & Engineering Chemistry Research*, 57:3443–3470, 2018.

[38] Air Liquide America Specialty Gases LLC. *Nitrogen | Specialty Pure Gas | Air Liquide*. Air liquide, 2015.

[39] J.M. Simon D.C. Dyson. A Kinetic Expression With Diffusion Correction For Ammonia Synthesis On Industrial Catalyst . *L & EC Fundamentals*, 7:605–610, 1968.

[40] B.Hansen A. Nielsen, J. Kjaer. Rate Equation and Mechanism of Ammonia Synthesis at Industrial Conditions . *Journal of Catalysis*, 3:68–79, 1964.

[41] J.T. Kummer P.H. Emmett. Kinetics of Ammonia Synthesis . *Industrial and Engineering Chemistry* , 35:677–683, 1943.

[42] E.Bahadori I. Rossetti A. Tripodi, M.Compagnoni. Process simulation of ammonia synthesis over optimized Ru/C catalyst and multibed Fe + Ru configurations . *Industrial and Engineering Chemistry* , 66:176–186, 2018.

[43] Environment agency Austria. Production of ammonia, nitric acid, urea and n-fertilizer. In *Umweltbundesamt*, 2017.

[44] A.A. Kiss A.C. Dimian, C.S. Bildea. Pinch Point Analysis. *Computer Aided Chemical Engineering*, 35:525–564, 2014.

[45] Rameshwar Sah and S. Dutta. *i) Direct Reduced Iron: Production*, pages pp 1082–1108. 03 2016.

[46] J. Goudman. *Cours de Sidérurgie*. Institut Gramme, école spéciale d'ingénieurs techniciens, 1957.

[47] F. Patisson A. Ranzani da Costa, D. Wagner. Modelling a new, low CO2 emissions, hydrogen steelmaking process. *Journal of Cleaner Production*, 46:27–35, 2013.

[48] B. Viswanatha M.V.C.Sastri, R.P.Viswanath. Studies on the reduction of iron oxide with hydrogen. *Int.J.Hydrogen Energy*, 7:951–956, 1982.

[49] D.Wagner. *Etude expérimentale et modélisation de la réduction du minerai de fer par l'hydrogène*. PhD thesis, Institut National Polytechnique de Lorraine, January 2008.

[50] H.Hamadeh. *Modélisation mathématique détaillée du procédé de réduction directe du minerai de fer*. PhD thesis, Institut National Polytechnique de Lorraine, June 2018.

[51] R.L. González, F.L. Acosta, M. Lowry, D. Kundrat, A. Wyatt, J. Kuntze, and H. Fuchs. Improvements in yield in an all-dri-fed eaf from minimization of feo generation during melting as well as post-reduction of feo from residual slag. *Iron and Steel Technology*, 15:36–41, 01 2018.

[52] R. V. Williams. *Control and Analysis in iron and Steelmaking*, chapter , page 121. Butterworth scientific, London, 1983.

[53] Y.Huang H.Yang C.Chou, F.Chen. Carbon Dioxide Capture and Hydrogen Purification from Synthesis Gas by Pressure Swing Adsorption. *The Italian Association of Chemical Engineering* , 32:1855–1860, 2013.

[54] K. A. Andreassen R. E.Stensrod C. A. Grande, R. Blom. Experimental Results of Pressure Swing Adsorption (PSA) for Precombustion CO2 Capture with Metal Organic Frameworks. *Energy Procedia*, 114:2265–2270, 2017.

[55] G. Li Y. Guo Y. Yang Z. Zhu, T. Jiang. *Thermodynamics of Reactions Among Al2O3, CaO, SiO2 and Fe2O3 During Roasting Processes* , chapter 30, pages 825–830. School of Minerals Processing and Bioengineering, Changsa, 2011.

[56] N. Zapuskalov. Comparison of Continuous Strip Casting with Conventional Technology. *ISIJ International*, 43:1115–1127, 2003.

[57] A. Jungbauer J. Penn, P. Pennerstorfer. New Generation of Continuous Casting Plants with Intelligent Manufacturing Strategy. *BHM*, 163:11–17, 2018.

[58] Ramesh Nayak. Continuous casting of steel and simulation for cost reduction. *Indian foundry journal*, 60:43–47, 08 2014.

[59] C. P. Bergmann J. A. S.Ten ório D.C.R.Espinosa M. C. da Silva, A. M. Bernardes. Characterisation of electric arc furnace dust generated during plain carbon steel production. *Iron working and steelmaking*, 35:315–320, 2008.

[60] R. Turton R. Bailie W. Whiting J. Shaeiwitz, D. Bhattacharyya. *Analysis, Synthesis, and Design of Chemical Processes*. Pearson, 2013.

[61] L. J. Nilsson V. Vogl, M. Ahman. Assessment of hydrogen direct reduction for fossil-free steelmaking. *Journal of Cleaner Production*, 203:736–745, 2018.

[62] L. Schrefler F. Genoese A. Marcu A. Renda J. Wieczorkiewicz S. Roth F. Infelise G. Luchetta L. Colantoni W. Stoefs J. Timini F. Simonelli C. Egenhofer, V. Rizos. *Composition and drivers of energy prices and costs in energy intensive industries: the case of ceramics, flat glass and chemical industries*. Center For European Policy Studies, 2014.

[63] Institute for Sustainable Process Technology ISPT. Feasibility study for the value chains and business cases to produce co2-free ammonia suitable for various market applications. 2017.

[64] W.M. Vatavuk. Updating the ce plant cost index. *Chemical Engineering*, 109:62–70, 01 2002.

[65] Economic Indicators. *Chemeng Online*, page 160, 2016.

[66] G. Léonard. *Introduction to economic analysis, application to industrial processes*. University of Liège, 2019.

[67] Informal discussion with M. Bertels Sales Engineer Research and Analysis. Air Liquide, December 4, 2019.

[68] Informal discussion with A. Hoxha, Technical Director. Fertilizers Europe, December 20, 2019.

[69] W. Huang. Impact of rising natural gaz prices on U.S. ammonia supply. *Economic research service*, pages 217–235, 2007.

[70] G. Luchetta F. Simonelli W. Stoefs J. Timini L. Colantoni V. Rizos, F. Infelise. *For a study on composition and drivers of energy prices and costs in energy intensive industries : the case of the chemical industry - Ammonia*. Center For European Policy Studies, 2014.

[71] European Commission. Eu emissions trading system (eu ets). https://ec.europa.eu/clima/policies/ets_en, accessed on November 27, 2019.

[72] Marketsinsider. Co_2 european emission allowances. https://markets.businessinsider.com/commodities/co2-european-emission-allowances, accessed on December 12, 2019.

[73] S. Schjolset. The msr: Impact on market balance and prices. In *Thomson Reuters*, 2014.

[74] J. Hermse. Dutch Government Plans CO2 Emissions Levy for Industrial Firms. www.bloomberg.com/articles/2019-06-28/dutch-government-plans-co2-emissions-levy-for-industrial accessed on January 12, 2020.

[75] B.G. Thomas. Continuous Casting (metallurgy). *Yearbook of Science and Technology*, pages 1–6, 2004.

[76] E. Pirard. *Mineral Ressources*. University of Liège, 2017.

[77] M. Le Gleuher M. Léguerinel. Le graphite naturel et synthétique. http://www.mineralinfo.fr/ecomine, accessed on October 17, 2019.

[78] Y. Charts. European union natural gas import price. https://ycharts.com/indicators/europe_natural_gas_price, accessed on November 24, 2019.

[79] Bourse. Cours de l'acier. https://www.boursorama.com/bourse/matieres-premieres/cours/_HR/, accessed on December 21, 2019.

[80] JDN. Prix des métaux : les tarifs des métaux en février 2020. https://www.journaldunet.fr/patrimoine/guide-des-finances-personnelles/1146972-prix-des-metaux-les-tarifs-des-metaux-en-fevrier\r-2020/, accessed on February 05, 2020.

[81] H. G. van Oss. Iron and Steel slag. *Mineral Commodity Summaries*, pages 86–87, 2019.

[82] Combustible Piron. Prix charbon. https://www.combustibles-piron.be/fr/charbons/index/categorie/10%20kg/, accessed on January 23, 2020.

[83] European Commission. Innovation Fund : Driving clean innovative technologies towards the market. , pages 1–17, 2019.